Research Article

HOXA11-AS aggravates microglia-induced neuroinflammation after traumatic brain injury

Xiang-Long Li[1, 2, 3], Bin Wang[1], Fu-Bing Yang[1], Li-Gang Chen[1, 2, 3, *], Jian You[1, 2, 3, *]

Graphical Abstract *Up-regulating HOXA11-AS aggravates the inflammatory response of microglia and astrocytes by down-regulating the miR-124-3p-MDK axis*
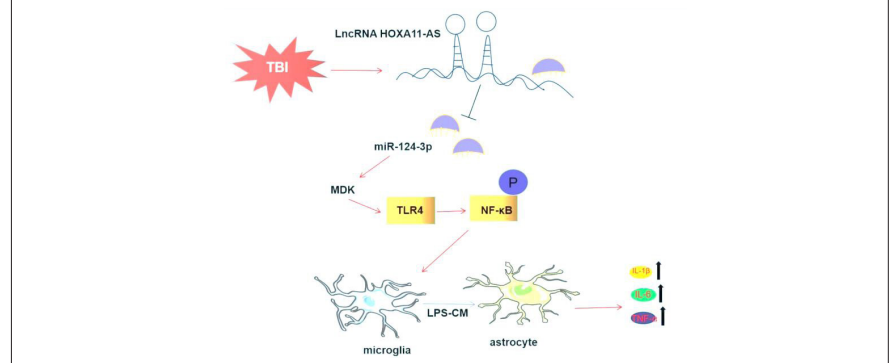
Abstract

Long noncoding RNAs (lncRNAs) participate in many pathophysiological processes after traumatic brain injury by mediating neuroinflammation and apoptosis. Homeobox A11 antisense RNA (HOXA11-AS) is a member of the lncRNA family that has been reported to participate in many inflammatory reactions; however, its role in traumatic brain injury remains unclear. In this study, we established rat models of traumatic brain injury using a weight-drop hitting device and injected LV-HOXA11-AS into the right lateral ventricle 2 weeks before modeling. The results revealed that overexpression of HOXA11-AS aggravated neurological deficits in traumatic brain injury rats, increased brain edema and apoptosis, promoted the secretion of proinflammatory factors interleukin-1β, interleukin-6, and tumor necrosis factor α, and promoted the activation of astrocytes and microglia. Microglia were treated with 100 ng/mL lipopolysaccharide for 24 hours to establish *in vitro* cell models, and then transfected with pcDNA-HOXA11-AS, miR-124-3p mimic, or sh-MDK. The results revealed that HOXA11-AS inhibited miR-124-3p expression and boosted MDK expression and TLR4-nuclear factor-κB pathway activation. Furthermore, lipopolysaccharide enhanced potent microglia-induced inflammatory responses in astrocytes. Forced overexpression of miR-124-3p or downregulating MDK repressed microglial activation and the inflammatory response of astrocytes. However, the miR-124-3p-mediated anti-inflammatory effects were reversed by HOXA11-AS. These findings suggest that HOXA11-AS can aggravate neuroinflammation after traumatic brain injury by modulating the miR-124-3p-MDK axis. This study was approved by the Animal Protection and Use Committee of Southwest Medical University (approval No. SMU-2019-042) on February 4, 2019.

Key Words: astrocyte; competitive endogenous RNA; HOXA11-AS; microglia; midkine; miR-124-3p; neuroinflammation; traumatic brain injury

Chinese Library Classification No. R446; R741.02; R364.5

Introduction

Traumatic brain injury (TBI) causes a large number of deaths and permanent disability that are related to the progression of secondary brain injury and bleeding, which results in elevated morbidity and mortality (Yang et al., 2019c). However, the pathophysiological heterogeneity of TBI hinders development of treatments. In physiological conditions, neurons, glial cells, the neurovascular unit, and extracellular matrix influence complex synaptic plasticity mechanisms and balance the central nervous system's (CNS) microenvironment by controlling multiple biological processes, including neural stem cell differentiation, neuronal migration, cellular composition, glial proliferation, and astrocyte phenotypes (Barros et al., 2011; Ceci et al., 2018; Lam et al., 2019; De Luca et al., 2020). Following TBI, microglia and astrocytes become activated; this results in the overproduction of neuroinflammatory mediators that greatly aggravate TBI (Kabadi et al., 2014; Sharma et al., 2020). Therefore, uncovering TBI's specific mechanisms could help to identify therapeutic targets for TBI treatment.

Long noncoding RNAs (lncRNAs) are a class of noncoding RNAs longer than 200 nucleotides that lack a protein-coding function; lncRNAs play a vital role in human physiology and are associated with many cancer types (Yang et al., 2019a; Gong et al., 2020; Liu et al., 2020; Zhang et al., 2020; Di et al., 2021).

[1]Department of Neurosurgery, the Affiliated Hospital of Southwest Medical University, Luzhou, Sichuan Province, China; [2]Neurosurgical Clinical Research Center and Academician (Expert) Workstation of Sichuan Province, Luzhou, Sichuan Province, China; [3]Laboratory of Neurological Diseases and Brain Functions, the Affiliated Hospital of Southwest Medical University, Luzhou, Sichuan Province, China
*Correspondence to: Jian You, MD, dr_you00@163.com; Li-Gang Chen, ligangchen86@163.com.
https://orcid.org/0000-0003-3979-3696 (Jian You)

lncRNAs are also abnormally expressed following TBI and contribute to various pathophysiological processes after TBI by mediating neuroinflammation and apoptosis (Yu et al., 2017; Li et al., 2019b; Zhang et al., 2019). Homeobox A11 antisense RNA (HOXA11-AS) is an lncRNA that has been associated with various carcinomas (Li et al., 2017). HOXA11-AS has been shown to aggravate inflammatory disease progression. For example, HOXA11-AS promoted the inflammatory response in vascular cells via phosphatidylinositol 3-kinase/protein kinase B (PI3K/Akt) pathway activation, leading to diabetic arteriosclerosis (Jin et al., 2018). In another study of CaOx crystal-induced kidney inflammation, HOXA11-AS enhanced kidney inflammation by modulating the miR-124-3p/macrophage cationic peptide 1 axis (Li et al., 2020). However, the role of HOXA11-AS in TBI has not yet been explored.

Similar to lncRNAs, microRNAs (miRNAs, small, single-stranded RNAs with about 22–25 nucleotides) are a class of endogenous noncoding RNAs. A previous study confirmed that miRNAs shuttled by extracellular vesicles play an essential role in glia-neuron communication, and also affect inflammation in the CNS microenvironment (Prada et al., 2018). In addition, TBI-induced alterations in miRNAs affect the blood-brain barrier, neuroinflammatory response, hippocampal neurogenesis, and neurological recovery in TBI rats (Yang et al., 2019d; Wu et al., 2020). Interestingly, miR-124-3p was found to be significantly elevated in the serum of patients with TBI, and could thus be used as a blood biomarker for TBI (O'Connell et al., 2020). Furthermore, Vuokila et al. (2020a) confirmed that the miR-124-3p level was higher in the plasma of Sprague-Dawley rats 2 days after TBI, and the lesion area was more extensive at the chronic time point compared with normal rats. Hence, miR-124-3p has an abnormal expression after TBI, but the specific mechanism of miR-124-3p following TBI remains unclear.

Midkine (MDK) is a heparin-binding growth factor involved in many physiological processes, including neurotrophic and neurite growth activity (Winkler and Yao, 2014). Recent studies have shown that MDK and MDA inhibitors may act as therapeutic agents in inflammatory CNS diseases involving enhanced leukocyte migration and neuroinflammation (Muramatsu, 2011; Vicente-Rodríguez et al., 2016). Therefore, it is possible that MDK regulates neuroinflammatory responses in TBI.

lncRNA can function as a competitive endogenous RNA to sponge miRNA, and then participate in the expression regulation of target genes (Tay et al., 2014). However, the specific mechanism of HOXA11-AS/miR-124-3p/MDK in TBI remains to be studied. This study investigated the role of HOXA11-AS in modulating the inflammatory responses of microglia and astrocytes, and explored the molecular mechanism of HOXA11-AS/miR-124-3p/MDK in a rat model of TBI.

Materials and Methods
Animals and grouping
The Animal Experiment Center of Southwest Medical University (license No. SCXK (Chuan) 2018-17) supplied 120 male Sprague-Dawley rats (8–10 weeks old, weight 220–250 g, specific-pathogen-free level) and 40 newborn Sprague-Dawley rats (weight 5–8 g, specific-pathogen-free level). Adult rats were housed in cages with *ad libitum* access to food and water, an ambient temperature of 20–25°C and a humidity of 50–52%, and a 12-hour light and 12-hour dark cycle. Animals had no access to food and water 12 hours before surgery. The adult rats were randomly divided into four groups, namely the sham (n = 10), TBI (n = 50), TBI + LV-NC (n = 30), and TBI + LV-HOXA11-AS groups (n = 30). The experimental design is shown in **Figure 1**. The Animal Protection and Use Committee of Southwest Medical University approved the experiment (approval No. SMU-2019-042) on February 4, 2019.
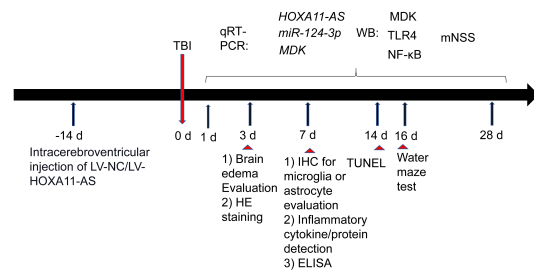

Figure 1 | **Animal experimental procedure diagram.**
HE: Hematoxylin and eosin; HOXA11-AS: Homeobox A11 antisense RNA; IHC: immunohistochemistry; LV: lentivirus vectors; miR-124-3p: microRNA-12-3p; MDK: midkine; mNSS: Modified Neurological Severity Score; NC: negative control; NF-κB: nuclear factor kappa-B; qRT-PCR: quantitative reverse transcription polymerase chain reaction; TBI: traumatic brain injury; TLR4: Toll like receptor 4.

TBI model establishment
The Feeney's method was adopted to prepare craniocerebral trauma models in rats (Feeney et al., 1981) using a weight-drop hitting device (ZH-ZYQ, Electronic Technology Development Co., Xuzhou, China). General anesthesia was administered through the abdominal cavity with a volume fraction of pentobarbital sodium (30 mg/g body weight; Sigma-Aldrich Corp., St. Louis, MO, USA) on an electric blanket. A 1.50 cm scalp incision was made in the middle of the skull, and a 5-mm bone window was opened on the left side of the sagittal suture, between the coronal suture and the herringbone suture. A 20 g weight was dropped from a height of 20 cm to hit the bone window with a sterilized impact needle. After the impact, we closed the bone window using bone wax and sutured the scalp. Finally, the rats were placed next to an electric stove for a 1-hour observation period and returned to their cage after resuscitation. Rats in the sham group did not receive the weight-dropped injury, and all other procedures were the same as for the other groups.

Modified Neurological Severity Score
The modified Neurological Severity Score (mNSS) was used to assess neurological function in each group (Long et al., 2020). The scoring scale includes motor function tests (muscle state and abnormal activity), sensory function tests (vision, touch, and proprioception), physiological reflex tests, and balance ability tests, and is suitable for assessing long-term neurological function after cerebral hypoperfusion. Five rats in each group were scored on days 1, 3, 7, 14, and 28 after modeling. The score of the scale ranged from 0 to 18 (normal score, 0; maximal deficit score, 18). If the rats could not perform the test or failed to react as expected, they earned one point.

Morris Water Maze test
At 15 days after modeling, the spatial learning and memory of rats were tested using the Morris Water Maze test (n = 10 in each group). The water maze (XR-XM101, Shanghai Xinruan Information Technology Co. Ltd., Shanghai, China) was a round pool (120 cm in diameter, 50 cm in height, and 31 cm in depth) with a water temperature of 24 ± 1°C. We divided the pool into four quadrants and placed a circular platform (10 cm in diameter, 30 cm in height, and 1 cm below the surface) in the second quadrant 20 cm from the pool wall, which was lower than the horizontal surface. The reference around the pool remained unchanged during the experiment. The motion tracking of experimental rats was recorded by the image acquisition system above the water maze. The two following assessments were performed: 1) Assessment of spatial learning ability: On the 7th day after the TBI operation, the rats were put into the water facing the pool wall from different quadrants each time, and the time (incubation period) taken

Research Article

for the rats to climb onto the platform (target quadrant time) was recorded. When rats failed to find the platform within 120 seconds, they were guided to the platform and stayed there for 20 seconds, and the incubation period was recorded as 120 seconds. The average incubation period after daily training (latency time) was calculated; 2) Spatial memory evaluation: Twenty-four hours after the assessment of learning ability, the platform in the second quadrant was removed, and rats were put into the water facing the wall from the four quadrants, respectively. The rats' platform crossing time (the second quadrant where the platform was located) was recorded.

Dry and wet method for measuring brain edema
The dry and wet weight method was performed to determine the water content of brain tissues (Long et al., 2020). On the 3rd day after modeling, the ischemic-side brain tissue was removed, and its wet weight was quickly measured. The dry weight was measured after 48 hours in an oven (BPG-9040A, GYPEX, Nanjing, China) at 105°C. The water content in brain tissue was calculated using the following formula: Brain water content (%) equals to the ratio of (wet weight – dry weight) to wet weight × 100.

Lentiviral vector construction and intracerebroventricular injection
Shanghai GenePharma Co., Ltd. (Shanghai, China) synthesized the lentivirus vectors of LV-NC and LV-HOXA11-AS. Two weeks before surgery, rats were anesthetized (pentobarbital sodium, 30 mg/body weight), and 4 μL LV-HOXA11-AS (50 μM) was injected using a stereotactic locator (XR-XM101, Shanghai Xinruan Information Technology Co. Ltd., Shanghai, China), and LV-NC was used as a blank control. Each rat was injected three times in the right lateral ventricle (front 0.3 mm, back 1.9 mm, side 3 mm, depth 1.8 mm). A 10-μL microsyringe (Zinsser Analytic, Frankfurt, Germany) was used for injections, and the injection rate was 0.1 μL/min.

TdT-mediated dUTP nick-end labeling staining
We collected rats' hippocampal tissues 14 days after modeling for TdT-mediated dUTP nick-end labeling (TUNEL) staining, and performed the experiment according to the TUNEL kit (Cat# TUN11684817, Roche Diagnostic Systems, Inc., Branching, NJ, USA). First, the slices were baked at 60°C for 15 minutes, dewaxed (by xylene), and dehydrated (by gradient ethanol). Second, the slices were treated with protease K (10 minutes, room temperature) and incubated (37°C, 1 hour) with the addition of prepared TUNEL reaction working solution. Next, the slices were treated with 3% H_2O_2 methanol, and the solution was left for 10 minutes (room temperature). We added the invert peroxidase solution and cultured the slices (37°C, 30 minutes). Next, diaminobenzidine was used for staining the slices. When re-staining with hematoxylin, the slices were dehydrated with gradient ethanol, cleaned with xylene, and sealed with resin. The TUNEL-positive cells were observed as yellow-brown under an optical microscope (Leica Camera, Solms, Germany). Apoptosis rate (%) = positive cell number/total cell number × 100.

Enzyme-linked immunosorbent assay
After the cortex had been weighed, we added the tissues with radio-immunoprecipitation assay lysis buffer (Beyotime) containing protease inhibitor (Cocktail, Roche Diagnostic Systems, Inc., Basel, Switzerland) for homogenization, performed centrifugation (5000 × g, 25 minutes, 4°C), and saved the supernatant. Interleukin-6 (IL-6), interleukin-1β (IL-1β), tumor necrosis factor alpha (TNF-α) and enzyme-linked immunosorbent assay kits (Abcam, Shanghai, China) were used to detect the concentrations of IL-1β, IL-6, and TNF-α in brain tissues, according to the manufacturer's guidelines.

Hematoxylin and eosin staining and immunohistochemistry
At the 3rd day post injury, the brain of rats in each group were isolated, fixed with 4% paraformaldehyde for 24 hours, then embedded in paraffin and sectioned (4-μm-thick slices). Next, the sections were dewaxed, covered with water, immersed in 100%, 90%, 80%, and 70% alcohol for 5 minutes each, and rinsed with water for 5 minutes. Then, the sections were respectively dyed with hematoxylin (for 5 minutes), washed with water, and stained with eosin (for 1 minute). After dehydration with 70%, 80%, 90%, and 100% alcohol for 10 seconds each, and xylene for 1 minute, neutral gum was used to seal the film. Finally, the sections were observed under a light microscope (Olympus, Tokyo, Japan). For immunohistochemistry, the dewaxed sections underwent antigen retrieval (0.01 M citrate buffer (pH 0.6; Cat#AR0024, Boster, Wuhan, China), were sealed with 5% goat serum, and incubated with rabbit anti-ionized calcium binding adapter molecule 1 (Iba1) (1:400, Cat# ab178846, RRID: AB_2636859, Abcam, Cambridge, UK) or rabbit anti-glial fibrillary acidic protein (GFAP, 1:500, Cat# ab68428, RRID:AB_1209224, Abcam) overnight at 4°C. Twelve hours later, the sections were incubated with goat anti-rabbit secondary antibody (1:1000, Cat# ab205718, Abcam) for 2 hours at room temperature, followed by staining with diaminobenzidine. Next, the nuclei of the cells were stained by hematoxylin (H810910, Macklin, Shanghai, China). Finally, the BX53 optical microscope was used to observe the staining.

Culture of primary microglial cells
We followed the specific method of Long et al. (2020). In brief, the cerebral cortexes of newborn rats (inhalation anesthesia via 2% isoflurane (Henan Tianfu Chemical Co., Ltd., Zhengzhou, China) and sacrifice by decapitation) were excised, cut into pieces, trypsinized (0.125% trypsin, Beyotime, Shanghai, China), filtered, and centrifuged. Then, the supernatant was discarded, and the cells were inoculated in a pre-coated poly-lysine culture flask with the addition of high glucose Dulbecco's Modified Eagle Medium (Gibco, Grand Island, NY, USA) containing 20% fetal bovine serum (Gibco). The cells were placed in a T75 culture flask in an incubator (37°C, 5% CO_2) and observed under an optical microscope (Leica Camera). After 7–9 days, the flasks were placed on a 200-r/min shaker for 4 hours when obvious layering of cells appeared. The culture medium containing microglia was collected and seeded in 6-well poly-lysine pre-coated plates. Finally, 100 ng/mL lipopolysaccharide (LPS) was used to induce microglial cells for 24 hours and activate the primary microglial cells. The culture medium of microglia was harvested, subjected to centrifugation (170 × g for 10 minutes), and the suspended cells or debris were removed.

Culture of primary astrocytes
We followed the specific method of a previous study (Witcher et al., 2021). Briefly, the cerebral cortexes of newborn rats' brains were excised, cut into pieces, trypsinized (0.125% trypsin), filtered, and centrifuged. After the supernatant had been discarded, Dulbecco's Modified Eagle Medium high-glucose medium containing 20% fetal bovine serum was added, and the cells were inoculated on a pre-coated poly-lysine culture plate (37°C, 5% CO_2). Primary astrocytes were identified by GFAP immunofluorescence, and the purity of astrocytes was over 95%. The microglia culture medium different groups (the control group and LPS group) underwent centrifugation (170 × g for 10 minutes, TGL16M, Gaoco, Changzhou, China). The supernatant was incubated with astrocytes for 24 hours.

Cell transfection
Shanghai GenePharma Co., Ltd. manufactured the pcDNA

empty vector (NC), pcDNA-HOXA11-AS (HOXA11-AS), miRNA control (miR-NC), miR-124-3p mimic, sh-NC, and sh-MDK. Primary microglial cells were inoculated onto 24-well plates (3×10^5 cells/well in density), and then incubated at 37°C for 24 hours (5% CO_2). In line with the supplier's instructions, we used Lipofectamine® 3000 (Invitrogen, Thermo Fisher Scientific, Inc., Carlsbad, CA, USA) to transfect NC, pcDNA-HOXA11-AS, miR-NC, miR-124-3p mimic, sh-NC, or sh-MDK into the primary microglial cells. The levels of HOXA11-AS and miR-124-3p in the cells were determined using quantitative reverse transcription polymerase chain reaction (qRT-PCR) to ensure transfection efficiency. Cells were further incubated at 37°C with 5% CO_2.

Immunofluorescence

The treated cells were trypsinized and re-inoculated in 24-well plates. After incubation (37°C, 5% CO_2, 48 hours), 4% paraformaldehyde was used to secure the cells at room temperature (20 minutes), and 3% H_2O_2 was used for endogenous peroxidase blocking for 15 minutes. Next, the cells were sealed with 5% goat serum (Beyotime) for 1 hour and cultured overnight with primary antibodies, including mouse anti-OX42 (CD11b + CD11c) (1:500, Cat# ab1211, RRID: AB_442947, Abcam), and rabbit anti-GFAP (1:500, Cat# ab68428, RRID: AB_1209224, Abcam), at 4°C. After being washed by cold phosphate buffer saline (PBS), the cells were incubated with goat anti-mouse IgG H&L (Alexa Fluor® 488) (1:200, Cat# ab150113, Abcam) or goat anti-rabbit IgG H&L (Alexa Fluor® 647) (1:200, Cat# ab205718, RRID: AB_2819160, Abcam) at room temperature for 1 hour. The nucleus was stained with 4',6-diamidino-2-phenylindole (Beyotime Biotechnology, Wuhan, China). Finally, a fluorescence microscope (Leica Camera) was used for observation and image collection. The quantification of the optical density of these markers was analyzed using ImageJ (National Institutes of Health, Bethesda, MD, USA).

qRT-PCR

After the total RNA of primary cultured cells of the rat cortex had been extracted using TRIzol reagent (Cat# 15596026, Invitrogen) and the concentration detected, complementary DNA was reverse-transcribed according to the TaKaRa kit's instructions (Cat# RR047AA, Takara Bio Inc., Beijing, China) and then amplified for detection. Shanghai Sangon Biological Co., Ltd. synthesized the primers; the primer sequences are shown in **Table 1**. Reaction conditions were as follows: 95°C pre-denaturation for 30 seconds, 95°C denaturation for 5 seconds, and 60°C annealing/extension for 30 seconds, for a total of 40 cycles. The target gene's relative expression was calculated using the $2^{-\Delta\Delta CT}$ method (ΔCT = target gene – β-actin, $\Delta\Delta$ = ΔCT experiment – ΔCT control).

Table 1 | Primers used in this study

Genes	Forward primers (5'–3')	Reverse primers (5'–3')
HOXA11-AS	CTC CTT GTT AGC CGT TTC CG	TGT GTC TGC AGA GAA GGG AG
MiR-124-3p	AAG TAC TCT AAG GCA CGC GGT	CAG TGC AGG GTC CGA GGT
MDK	TGT GGG GAA CAA AAG CG	TGC CTT CTG TCT GCT CGT TA
IL-6	GGA GCC CAC CAA GAA CGA TA	CAG GTC TGT TGG GAG TGG TA
TNF-α	GGA TTA TGG CTC AGG GTC CA	ACA TTC GAG GCT CCA GTG AA
IL-1β	GGC TCA TCT GGG ATC CTC TC	TCA TCT TTT GGG GTC CGT CA
GAPDH	GCT CTC TGC TCC TGT TC	ACG ACC AAA TCC GTT GAC TC
U6	CGC TTC GGC AGC ACA TAT AC	TTC ACG AAT TTG CGT GTC AT

GAPDH: Glyceraldehyde 3 phosphate dehydrogenase; HOXA11-AS: homeobox A11 antisense RNA; IL-6: interleukin-6; IL-1β: interleukin-1β; MDK: midkine; miR-124-3p: microRNA-12-3p; TNF-α: tumor necrosis factor-α.

Dual-luciferase reporter gene assay

The online database StarBase (http://starbase.sysu.edu.cn/index.php) was used to analyze the potential target genes of HOXA11-AS. According to the analysis results, Promega (Madison, WI, USA) constructed all luciferase reporting vectors (HOXA11-AS-WT, HOXA11-AS-MUT, MDK-WT, and MDK-MUT). We performed all experiments in triplicate and repeated them three times. The microglial cell line BV2 (4.5×10^4) (National Collection of Authenticated Cell Cultures, Shanghai, China) were inoculated in 48-well plates, and cultured until 70% confluence was reached. Then, HOXA11-AS-WT, HOXA11-AS-MUT, MDK-WT, MDK-MUT, and miR-124-3p mimic or negative control were co-transfected into BV2 cells using Lipofectamine 2000 (Cat# 11668030, Invitrogen). Forty-eight hours after transfection, luciferase viability was determined.

RNA immunoprecipitation assay

RNA-binding protein immunoprecipitation tests were performed using the Magna RNA immunoprecipitation Kit (Cat# 17-700, EMD MilliPore, Billerica, MA, USA) as per the supplier's instructions. After the cells had been lysed with RNA immunoprecipitation buffer, anti-Ago-2 antibody or IgG antibody was added for incubation overnight (4°C). The lysates were collected and the total RNA in the lysates was also isolated. Then, qRT-PCR was used to detect HOXA11-AS and MDK expression.

Western blot assay

After the tissues and cells had been treated, the supernatant was extracted, the protein lysates (Roche, Sigma-Aldrich, Shanghai, China) were added, and the total proteins separated. Fifty micrograms total protein was isolated by 12% polyacrylamide gel and underwent electrophoresis at a constant voltage of 100 V for 2 hours. Next, the protein was electrically transferred to polyvinylidene fluoride membranes. The membranes were then sealed with 5% skimmed milk powder (room temperature, 1 hour), washed three times with Tris HCl buffer solution containing 0.5% Tween-20 (10 minutes each time), and incubated at 4°C overnight with rabbit anti-MDK (1:1000, Cat# ab52637, RRID:AB_880698, Abcam), rabbit anti-aquaporin-4 (AQP4) (1:1000, Cat# ab46182, RRID:AB_955676, Abcam), rabbit anti-TLR4 (1:1000, Cat# ab13867, RRID:AB_300696, Abcam), rabbit anti-phosphorylation-NF-κB p65 (p-NF-κB p65, 1:1000, Cat# ab97726, RRID:AB_10681170,) Abcam, rabbit anti-NF-κB p65 (1:1000, Cat# ab16502, RRID:AB_443394, Abcam), and rabbit anti-β-actin (1:1000, Cat# ab8227, RRID:AB_2305186, Abcam). Tris HCl buffer solution containing 0.5% Tween-20 was used to wash the membranes. We then incubated the membranes with horseradish peroxidase-labeled anti-rabbit secondary antibody (1:2000, Cat# ab205718, RRID: AB_2819160, Abcam) at room temperature for 1 hour. Finally, we used Novex™ ECL Chemiluminescent Substrate Reagent Kit (Cat# WP20005, Invitrogen) to develop color, and ImageJ 1.44 software (National Institutes of Health, Bethesda, MD, USA) was used for optical density determination and analysis.

Statistical analysis

Data analysis was carried out using SPSS17.0 (SPSS Inc., Chicago, IL, USA). One-way analysis of variance with Tukey's *post hoc* test was used for the multivariate comparison, and an independent-sample *t*-test was used for between-group comparisons. Pearson's linear regression analysis was used to analyze the relationships between HOXA11-AS, miR-124-3p, and MDK expression in the brain of TBI rats. The data are presented as the mean ± standard deviation (SD). $P < 0.05$ was considered as statistically significant.

Research Article

Results

Expression of HOXA11-AS, miR-124-3p, and MDK in the injured cortex of TBI rats

We constructed a TBI rat model and performed qRT-PCR to evaluate the expression of *HOXA11-AS*, *miR-124-3p*, and *MDK* in TBI on days 1, 3, 7, 14, and 28. *HOXA11-AS* was upregulated in TBI rats ($P < 0.05$, **Figure 2A**), and *miR-124-3p* expression was decreased and reached its minimum on the 14th day ($P < 0.05$, **Figure 2B**) compared with the control group. Western blot and qRT-PCR revealed that MDK mRNA and protein expression was upregulated compared with the control group ($P < 0.05$; **Figure 2C** and **D**). According to the Pearson's analysis, miR-124-3p was negatively correlated with HOXA11-AS ($R^2 = 0.7593$, $P = 0.005$) and MDK ($R^2 = 0.5033$, $P = 0.0216$), while HOXA11-AS was positively correlated with MDK ($R^2 = 0.4261$, $P = 0.0408$; **Figure 2E–G**). These results indicated that HOXA11-AS, miR-124-3p, and MDK all play a role in TBI.
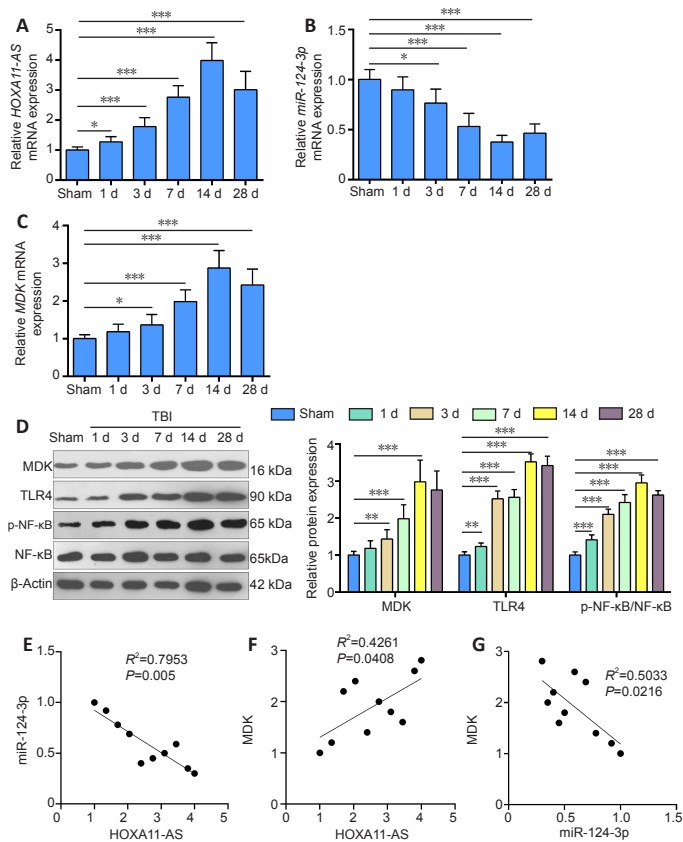

Figure 2 | Expression characteristics of HOXA11-AS, miR-124-3p, and MDK in the injured cortex of TBI rats.
(A–C) qRT-PCR detected the expression of *HOXA11-AS* (A), *miR-124-3p* (B), and *MDK* (C) mRNA in the injured cortex of TBI rats on days 1, 3, 7, 14, and 28 after injury. The target mRNA expression was normalized to the sham group. (D) Western blot was used to assess MDK, TLR4, and NF-κB protein expression in rat brain tissues on days 1, 3, 7, 14, and 28 after TBI. The target protein expression was normalized by the sham group. (E) Pearson analysis illustrated that HOXA11-AS is negatively correlated with miR-124-3p ($R^2 = 0.7593$, $P = 0.005$). (F) Pearson's analysis revealed that HOXA11-AS was positively correlated with MDK ($R^2 = 0.4261$, $P = 0.0408$). (G) Pearson's analysis revealed that miR-124-3p is negatively correlated with MDK ($R^2 = 0.5033$, $P = 0.0216$). Data are expressed as the mean ± SD ($n = 5$). All experiments were repeated three times. *$P < 0.05$, **$P < 0.01$, ***$P < 0.001$, *vs.* sham group (one-way analysis of variance with Tukey's *post hoc* test). HOXA11-AS: Homeobox A11 antisense RNA; MDK: midkine; TLR4: Toll like receptor 4; NF-κB: nuclear factor kappa-B; miR-124-3p: microRNA-12-3p.

Overexpression of HOXA11-AS aggravates brain edema, cognitive impairment, and apoptosis of neurons in TBI rats

To explore the effect of HOXA11-AS on TBI rats, we constructed a rat model with an overexpression of HOXA11-AS, which was subsequently verified by qRT-PCR to be highly expressed in rat brain tissues (**Figure 3A**). Moreover, we assessed the neurological functions of rats by mNSS and water maze test. The mNSS of rats in the TBI group was significantly higher compared with the sham group ($P < 0.05$; **Figure 3B**). The latency period of TBI rats to find the platform in the water maze test was prolonged, and the residence time of rats in the platform quadrant and the frequency they crossed the platform were lower than those in sham group rats ($P < 0.05$; **Figure 3C–E**). Nevertheless, HOXA11-AS upregulation increased the mNSS of TBI rats, enhanced the time spent searching for the platform, reduced the residence time of rats in the platform quadrant, and reduced the frequency of platform crosses ($P < 0.05$; **Figure 3B–E**). On the third day after modeling, the rats' brain water content was measured using the dry and wet method and hematoxylin and eosin staining. The brain water content was significantly higher in the TBI rats compared with the sham group, which was further aggravated by HOXA11-AS upregulation ($P < 0.05$; **Figure 3F–G**). Finally, TUNEL staining was used to identify cell apoptosis. Compared with the sham group, the number of TUNEL-positive cells in the TBI group increased remarkably, while overexpression of HOXA11-AS resulted in a further increase in TUNEL-positive cells ($P < 0.05$; **Figure 3H**). These results indicated that overexpression of HOXA11-AS aggravated the neurological deficits of TBI rats.

HOXA11-AS increases microglial cell activation and the inflammatory response in TBI rats

Multiple studies have shown that neuroinflammation is a major secondary injury mechanism of TBI (Long et al., 2020). First, Iba1-labeled microglia and GFAP-labeled astrocytes in brain tissues of TBI rats were detected via immunohistochemistry and western blot. Compared with the sham group, numbers of Iba1-positive microglia and GFAP-positive astrocytes were significantly higher in the TBI group, and this effect was further increased by HOXA11-AS overexpression ($P < 0.05$, **Figure 4A–D**). Second, the levels of IL-1β, IL-6, and TNFα were verified by enzyme-linked immunosorbent assay. We found that all of the inflammatory cytokines were upregulated in the TBI group. When HOXA11-AS was upregulated, IL-1β, IL-6, and TNF-α were further upregulated in the TBI + LV-HOXA11-AS rats ($P < 0.05$, *vs.* TBI group; **Figure 4E**). Finally, western blot was used to detect MDK and AQP4, and their expression in the TBI group was upregulated, while MDK and AQP4 levels in the HOXA11-AS group were even more increased (compared with the sham group) ($P < 0.05$, **Figure 4F**). These results suggest that the overexpression of HOXA11-AS increased microglia and astrocyte activation and the release of inflammatory factors following TBI lesions.

Activated microglia enhance the activation of astrocytes

We performed immunofluorescence to detect microglial activation (labeled by OX42). We found that OX42 expression in microglia cells significantly increased after LPS stimulation ($P < 0.05$, **Figure 5A**). In addition, qRT-PCR results illustrated elevated expression of TNF-α, IL-1β, and IL-6 in microglia (**Figure 5B**), and the protein levels of MDK, TLR4, and phosphorylated NF-κB in microglia were also upregulated after LPS treatment ($P < 0.05$; **Figure 5C** and **D**). We then used the microglial culture medium to incubate with the primary astrocytes, and found that the condition medium from microglia in the LPS group induced remarkable activation of astrocytes (labeled by GFAP staining) ($P < 0.05$; **Figure 5E**). The mRNA levels of IL-1β, IL-6, and TNF-α in astrocytes were also upregulated by LPS, and even more upregulated by LPS-treated medium from microglia (**Figure 5F**). Finally, western blot was used to examine MDK, AQP4, and TLR4/NF-κB expression in astrocytes. The results revealed that LPS promoted MDK, AQP4, and TLR4/NF-κB expression in
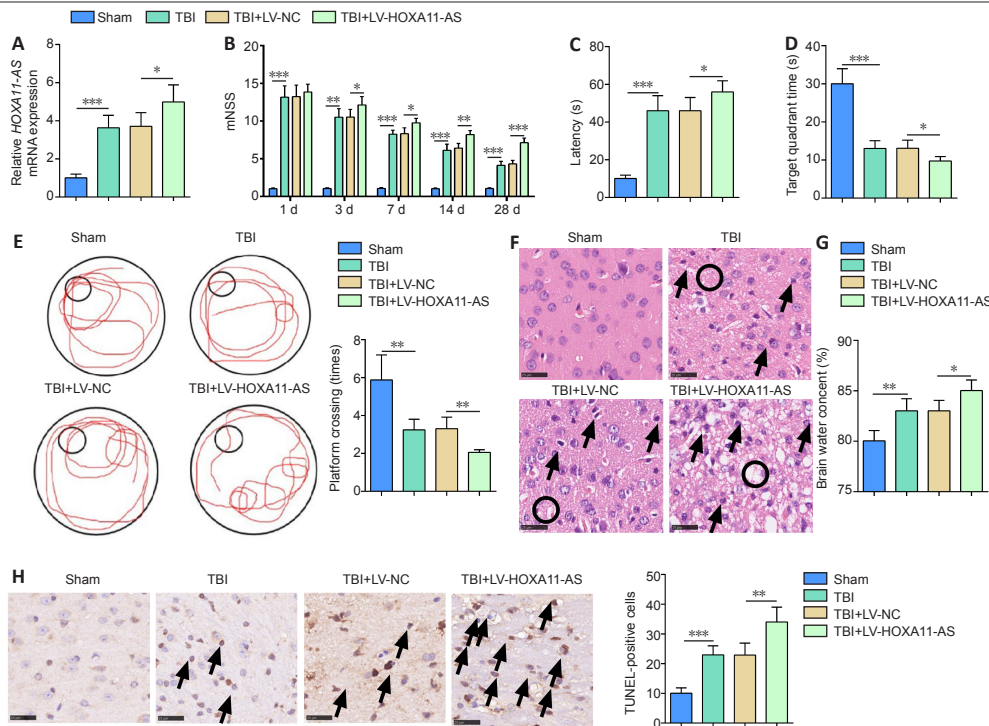
Figure 3 | HOXA11-AS overexpression aggravates brain edema, cognitive impairment, and neuronal apoptosis in TBI rats.
All rats were divided into the four following groups: sham group (sham operated group), TBI group, TBI + LV-NC group (negative lentivirus vector was injected into the right lateral ventricle of TBI rats), and TBI + HOXA11-AS group (HOXA11-AS lentivirus was injected into the ventricle of TBI rats). (A) qRT-PCR detected the expression of *HOXA11-AS*. The target mRNA expression was normalized by the sham group. (B) The rats' mNSS was measured on days 1, 3, 7, 14, and 28 (n = 10). (C–E) The water maze test was used to evaluate learning and memory abilities of TBI rats (n = 8). (C) Latency. (D) Target quadrant time. (E) Platform crossing times. (F) Hematoxylin and eosin staining was used to detect the pathological brain changes in rats at the 3rd day post injury; following TBI, obvious neuron injury (arrows) and tissue edema (circles) emerged, while overexpression of HOXA11-AS aggravated TBI-mediated pathological changes. (G) The dry and wet method was used to detect cerebral edema (n = 5). (H) TUNEL-positive cells (arrows) in the brain tissue of TBI rats were measured; TBI resulted in significant apoptotic neurons, and upregulating HOXA11-AS enhanced this change (n = 5). Scale bars: 50 μm. Data are expressed as the mean ± SD (n = 5). All experiments were repeated three times. *$P < 0.05$, **$P < 0.01$, ***$P < 0.001$ (one-way analysis of variance with Tukey's *post hoc* test). HOXA11-AS: Homeobox A11 antisense RNA; mNSS: Modified Neurological Severity Score; TBI: traumatic brain injury; TUNEL: TdT-mediated dUTP nick-end labeling.
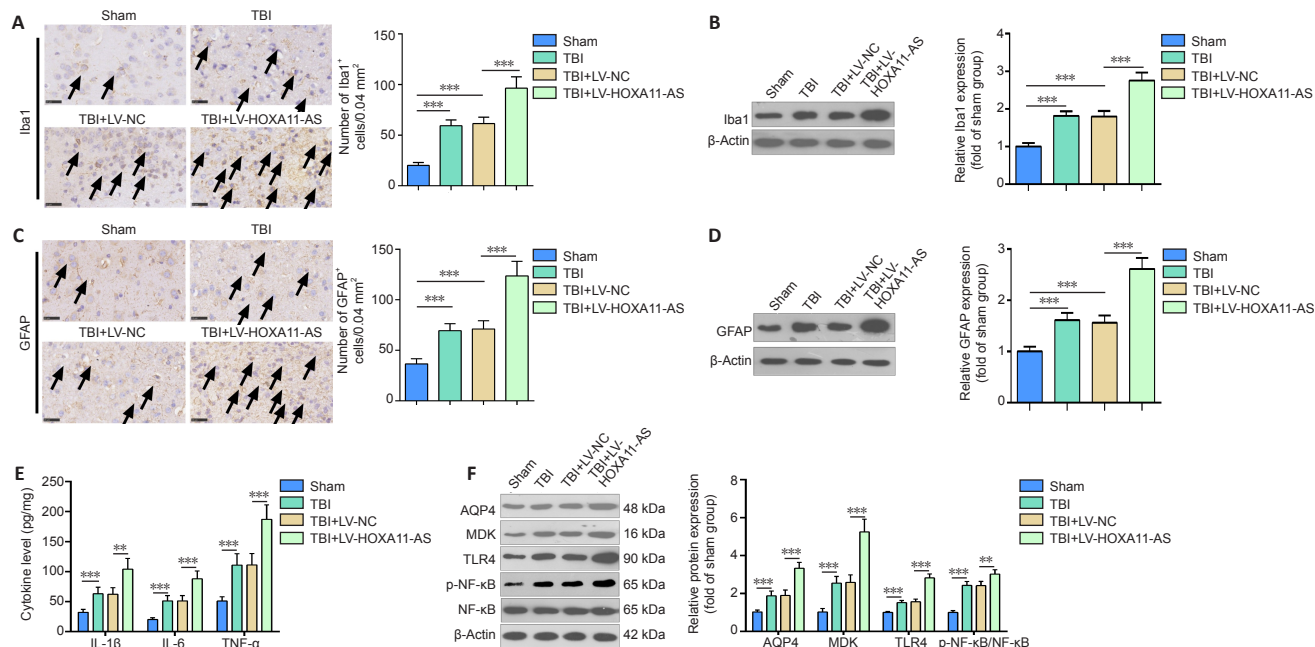

Figure 4 | HOXA11-AS increases microglia activation and the inflammatory response in TBI rats.
(A, B) Iba1-labeled microglia were detected using immunohistochemistry (A) and western blot (B). The TBI group had significantly more Iba1-positive cells compared with the sham group, and overexpression of HOXA11-AS1 further promoted the accumulation of Iba1-labeled microglia compared with the TBI + LV-NC group. (C, D) GFAP-labeled astrocytes were detected using immunohistochemistry (C) and western blot (D). The TBI group had significantly increased GFAP-positive cells, and overexpression of HOXA11-AS1 further promoted the accumulation of GFAP-labeled astrocytes. Arrows indicate positive cells. Scale bars: 50 μm. (E) ELISA was used to measure the expression of IL-1β, IL-6, and TNF-α. (F) Western blot was conducted to examine the protein expression of MDK, TLR4, NF-κB, and AQP4. The target protein expression was normalized by the sham group. Data are expressed as the mean ± SD (n = 5). All experiments were repeated three times. **$P < 0.01$, ***$P < 0.001$ (one-way analysis of variance with Tukey's *post hoc* test). AQP4: Aquaporin-4; ELISA: enzyme-linked immunosorbent assay; GFAP: glial fibrillary acidic protein; HOXA11-AS: Homeobox A11 antisense RNA; Iba1: ionized calcium binding adapter molecule 1; IL-1β: interleukin-1β; IL-6: interleukin-6; MDK: midkine; NF-κB: nuclear factor kappa-B; TBI: traumatic brain injury; TLR4: Toll like receptor 4; TNF-α: tumor necrosis factor-α.

astrocytes. Medium from microglia in the LPS group had even more significant effects in promoting those proteins (**Figure 5G**). These results indicate that LPS-activated microglia led to the activation of astrocytes by upregulating MDK-TLR4/NF-κB and inflammatory factors.

Overexpression of HOXA11-AS/miR-124-3p regulates the inflammatory response between microglia and astrocytes

MiR-124-3p mimic and/or HOXA11-AS overexpressing plasmids were transfected into microglia. qRT-PCR was used to detect gene expression, and revealed that HOXA11-AS was enhanced by LPS, while miR-124-3p had low expression levels in the LPS group compared with the control group (**Figure 6A** and **B**). However, miR-124-3p levels in the LPS + miR-124-3p + HOXA11-AS group were low compared with the LPS + miR-124-3p group (**Figure 6B**). Next, the inflammatory responses in microglia were assessed. The results indicated that overexpression of miR-124-3p inhibited LPS-induced proinflammatory cytokines and MDK and TLR4/NF-κB expression, while upregulation of HOXA11-AS mostly attenuated miR-124-3p-mediated effects (**Figure 6C–E**). The microglia-astrocyte interaction was also examined; compared with the LPS + miR-NC group, GAFP expression in astrocytes was significantly reduced after the upregulation of miR-124-3p (**Figure 6F**). In addition, the expression of *TNF-α*, *IL-1β*, and *IL-6* in astrocytes was evaluated using qRT-PCR, and revealed that overexpressing miR-124-3p in microglia significantly reduced the expression of *IL-1β*, *IL-6*, and *TNF-α* in astrocytes (**Figure 6G**). Furthermore, the expression of MDK, TLR4/NF-κB, and AQP4 in astrocytes was also significantly reduced following the upregulation of miR-124-3p (**Figure 6H**). Consistent with the results in microglia, upregulation of HOXA11-AS abolished miR-124-3p mimic-mediated anti-inflammatory functions in astrocytes (**Figure 6F–H**). These findings indicate that overexpression of miR-124-3p alleviated the activated microglia-mediated inflammatory response in astrocytes.

Downregulation of MDK induces a microglia-astrocyte inflammatory response via repression of miR-124-3p

To further clarify how MDK regulates microglia and astrocyte activation, we constructed a MDK-downregulated cell model in microglia (**Figure 7A**), which was then treated with LPS. Compared with the LPS + sh-NC group, TNF-α, IL-1β, IL-6, MDK, TLR4, and phosphorylated NF-κB levels declined significantly in the LPS + sh-MDK group (**Figure 7B–D**). Next, we treated astrocytes with medium derived from microglia. We found that astrocytic activation (labeled by GFAP), the levels of TNF-α, IL-1β, and IL-6, and protein expression of MDK, AQP4, TLR4, and phosphorylated NF-κB in astrocytes were all reduced compared with those seen in the LPS + sh-NC group (**Figure 7E–G**). Therefore, downregulation of MDK repressed microglia-induced astrocyte activation.

miR-124-3p is the target of HOXA11-AS and MDK

We browsed StarBase to identify potential target genes of HOXA11-AS, which revealed that HOXA11-AS targets miR-124-3p, and MDK is a potential target of miR-124-3p (**Figure 8A**). To determine the relationship between the three molecules, we conducted a dual-luciferase reporter gene experiment. The results indicated that miR-124-3p mimic notably decreased the luciferase activity of BV2 microglial cells transfected with HOXA11-AS-WT and MDK-3'-UTR-WT, but had no significant effect on the luciferase activity of mutant HOXA11-AS (HOXA11-AS-MUT) or MDK (MDK-MUT) (**Figure 8B** and **C**). Furthermore, to clarify the relationship between HOXA11-AS, miR-124-3p, and MDK, a RNA immunoprecipitation experiment was conducted. After transfection of miR-124-3p mimic in BV2 microglia cells, HOXA11-AS and MDK levels were both higher in the Ago2 antibody group compared with the IgG group, which suggests that HOXA11-AS and MDK bind to the Ago2 protein through miR-124-3p (**Figure 8D** and **E**). Taken together, these two experiments confirmed that HOXA11-AS sponged miR-124-3p, which then targeted the 3'-untranslated region of MDK.
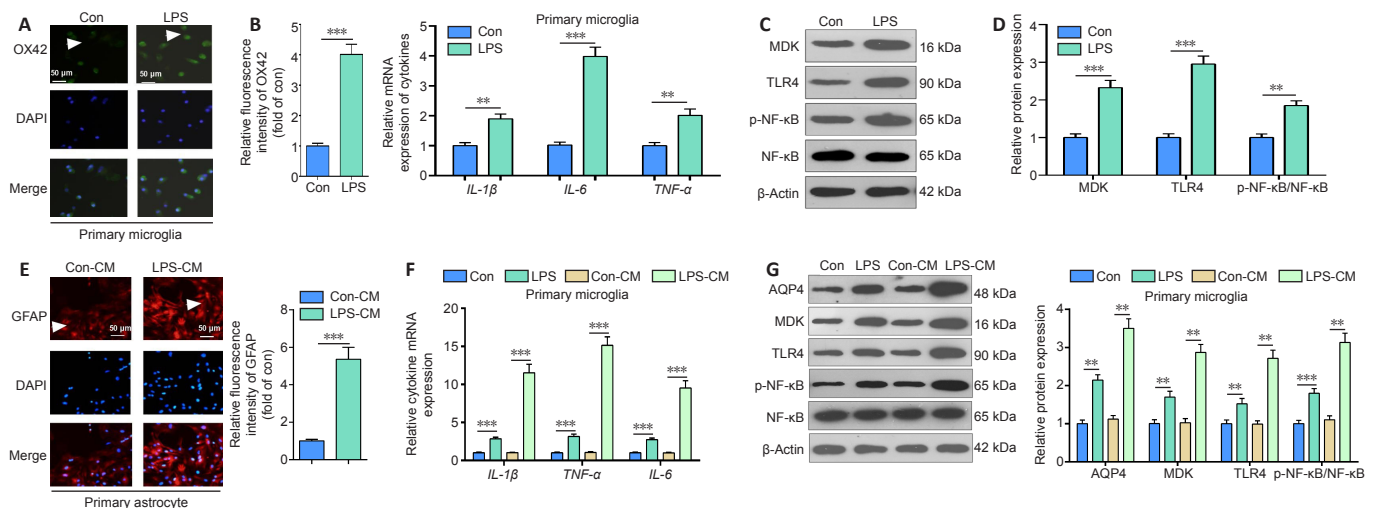

Figure 5 | Activated microglia promote the activation astrocytes.
Lipopolysaccharide (LPS; 100 ng/mL) was applied to microglial cells for 24 hours to activate the primary microglial cells. The condition medium of microglia was collected and then treated with astrocytes for 24 hours. (A) Cellular immunofluorescence detection of OX42 in primary microglia (green, stained by Alexa Fluor® 488, shown by arrow). LPS treatment enhanced OX42 expression and changed microglia from a multibranched shape (control group) into amoeba like shapes. (B) qRT-PCR was carried out to detect mRNA expression of inflammatory factors (including *IL-1β*, *IL-6*, and *TNF-α*) in microglia. The target mRNA expression was normalized to the expression level of the control group. (C, D) Western blot examined MDK, TLR4, and NF-κB protein expression in microglia. (E) Cellular immunofluorescence was performed to measure GFAP-labeled astrocytes (red, stained by Alexa Fluor® 647, shown by arrow). The condition medium from LPS-treated microglia enhanced GFAP expression in astrocytes, and promoted GFAP expression both in the cytoplasm and membrane. Scale bars: 50 μm. (F) qRT-PCR was used to detect mRNA expression of inflammatory factors (including *IL-1β*, *IL-6*, and *TNF-α*) in astrocytes. The target mRNA expression was normalized by the control group. (G) Western blot was used to measure the protein expression of MDK, TLR4, NF-κB, and AQP4 in astrocytes. The target protein expression was normalized by the control group. Data are expressed as the mean ± SD (*n* = 3). All experiments were repeated three times. **$P < 0.01$, ***$P < 0.001$ (one-way analysis of variance with Tukey's *post hoc* test). AQP4: Aquaporin-4; GFAP: glial fibrillary acidic protein; IL-1β: interleukin-1β; IL-6: interleukin-6; LPS: lipopolysaccharide; MDK: midkine; NF-κB: nuclear factor kappa-B; OX42: CD11b + CD11c; TLR4: Toll like receptor 4; TNF-α: tumor necrosis factor-α.
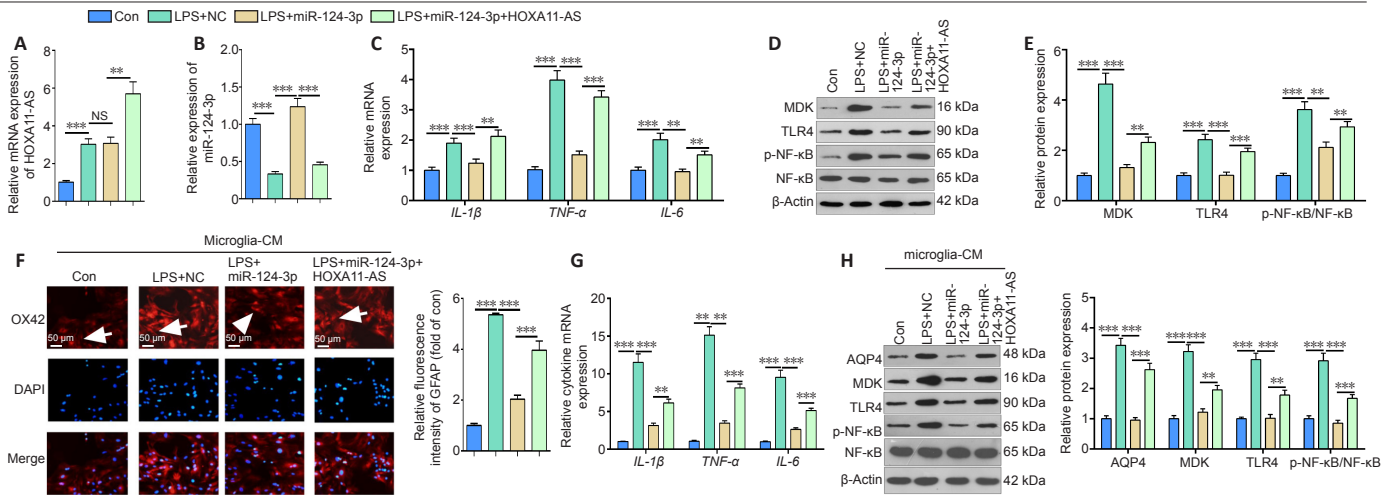
Figure 6 | Functions of HOXA11-AS/miR-124-3p in regulating the microglia-induced activation of astrocytes.
We applied miR-124-3p mimic and/or HOXA11-AS-overexpressing plasmids in primary microglia, then the condition medium of microglia was used to treat astrocytes. (A–C) qRT-PCR detection of gene expression of *HOXA11-AS* (A), *miR-124-3p* (B), and inflammatory factors (including *IL-1β*, *IL-6*, and *TNF-α*) (C). The target mRNA expression was normalized to the control group. (D, E) Western blot was used to examine MDK, TLR4, and NF-κB protein expression in microglia. The target was mRNA normalized to the control group. (F) Cellular immunofluorescence was used to detect GFAP (arrows, red, stained by Alexa Fluor® 647) in astrocytes. Compared with the con group, LPS treatment promoted GFAP expression in the cytoplasm and membrane, which was inhibited by miR-124-3p. However, upregulation of HOXA11-AS almost abolished the miR-124-3p-mediated effects. Scale bars: 50 μm. (G) qRT-PCR was used to detect gene expression of inflammatory factors. The target mRNA expression was normalized by the control group. Data are expressed as the mean ± SD (*n* = 3). All experiments were repeated three times. **P < 0.01, ***P < 0.001 (one-way analysis of variance with Tukey's *post hoc* test). AQP4: Aquaporin-4; GFAP: glial fibrillary acidic protein; HOXA11-AS: Homeobox A11 antisense RNA; IL-1β: interleukin-1β; IL-6: interleukin-6; LPS: lipopolysaccharide; MDK: midkine; miR-124-3p: microRNA-12-3p; NF-κB: nuclear factor kappa-B; OX42: CD11b + CD11c; TLR4: Toll like receptor 4; TNF-α: tumor necrosis factor-α.
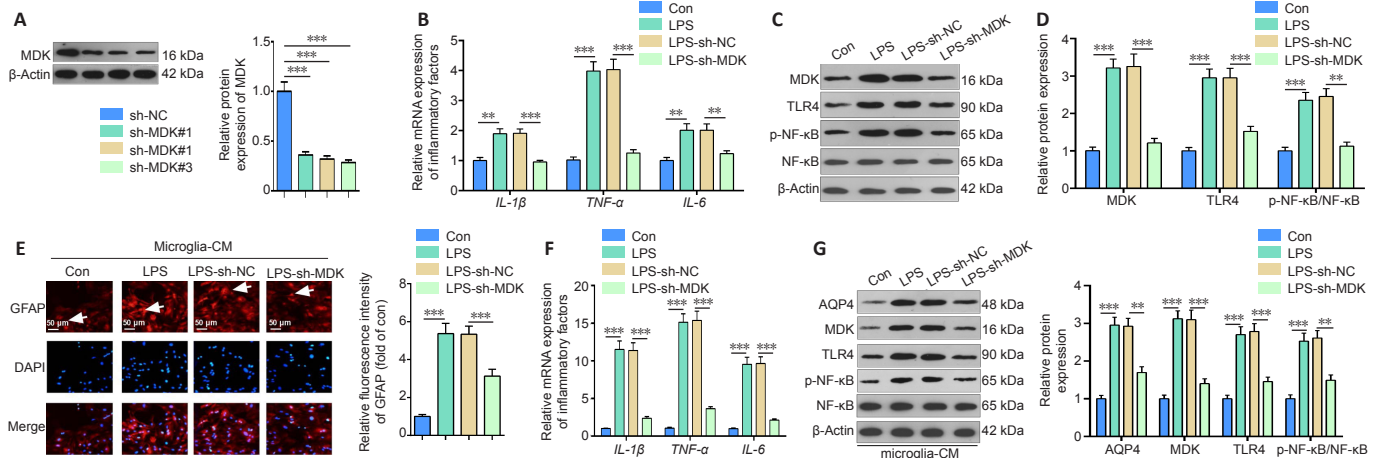

Figure 7 | Downregulation of MDK attenuates the microglia-induced activation of astrocytes.
The downregulated MDK model was constructed in primary microglia, and then the condition medium of microglia was used to treat astrocytes. (A) Western blot was used to detect MDK in microglia. The target protein expression was normalized by the sh-NC group. (B) Gene expression of inflammatory factors (including *IL-1β*, *IL-6*, and *TNF-α*) in microglia was determined using qRT-PCR. The mRNA protein expression was normalized by the sh-NC group. (C, D) Western blot was used to examine MDK, TLR4, and NF-κB protein expression in microglia. The target protein expression was normalized by the control group. (E) Cellular immunofluorescence was used to detect GFAP (red, stained by Alexa Fluor® 647, shown by arrows) in astrocytes. GFAP was mainly expressed in the cytoplasm and membrane. LPS enhanced GFAP expression in astrocytes, while knockdown of MDK reduced GFAP expression. Scale bars: 50 μm. (F) qRT-PCR was used to detect gene expression of inflammatory factors. mRNA expression was normalized by the control group. (G) Western blot was used to measure the protein expression of MDK, TLR4, NF-κB, and AQP4 in astrocytes. The target protein expression was normalized by the control group. Data are expressed as the mean ± SD (*n* = 3). All experiments were repeated three times. **P < 0.01, ***P < 0.001 (one-way analysis of variance with Tukey's *post hoc* test). AQP4: Aquaporin-4; con: control; GFAP: glial fibrillary acidic protein; HOXA11-AS: Homeobox A11 antisense RNA; IL-1β: interleukin-1β; IL-6: interleukin-6; LPS: lipopolysaccharide; MDK: midkine; miR-124-3p: microRNA-12-3p; NF-κB: nuclear factor kappa-B; OX42: CD11b + CD11c; TLR4: Toll like receptor 4; TNF-α: tumor necrosis factor-α.
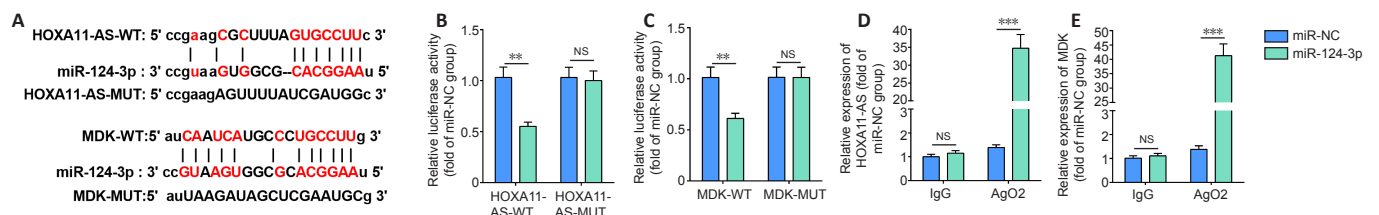
Figure 8 | miR-124-3p is the target of HOXA11-AS and MDK.
(A) Analysis of the upstream and downstream molecules of miR-124-3p using the StarBase database. (B, C) Luciferase-reporter gene assay was used to verify the binding relationship between miR-124-p and HOXA11-AS and MDK. (D, E) RNA immunoprecipitation was performed to detect the targeting relationship between miR-124-3p and HOXA11-AS and MDK. Data are expressed as the mean ± SD. All experiments were repeated three times. **P < 0.01, ***P < 0.001 (independent-sample *t*-test). HOXA11-AS: Homeobox A11 antisense RNA; MDK: midkine; miR-124-3p: microRNA-12-3p; MUT: mutant; WT: wild type.

Research Article

Discussion

This study investigated the effect of HOXA11-AS in TBI, and particularly its role in the cross-talk between microglia and astrocytes. We found that HOXA11-AS was overexpressed in a rat model of TBI. Forced upregulation of HOXA11-AS aggravated neuroinflammatory responses in astrocytes and microglia, and promoted neurological deficits in TBI rats. In addition, HOXA11-AS mediated the interaction between microglia and astrocytes via the miR-124-3p/MDK axis.

Several lncRNAs are known to be involved in craniocerebral diseases. Multiple lncRNAs are reportedly altered following TBI (Witcher et al., 2021). Meanwhile, many previous studies have demonstrated that silencing or overexpressing lncRNA promotes nerve repair in TBI rats (Yang et al., 2019b; Yi et al., 2019; Zhang et al., 2019). HOXA11-AS is a novel lncRNA that greatly contributes to glioblastoma as a novel regulator of human cancer and metastasis (Xue et al., 2018; Cheng et al., 2021). However, it has not been studied in the context of CNS inflammatory diseases. Here, we found HOXA11-AS was highly expressed in TBI rats and LPS-induced microglia. Highly-expressed HOXA11-AS increased TBI rats' cerebral edema, cognitive impairment, and neuronal apoptosis, and increased the microglia- and astrocyte-mediated inflammatory response.

Accumulating studies have revealed that miR-124-3p contributes to TBI development. For instance, one study found that the expression of miR-124-3p in microglia exosomes was upregulated after TBI, and the increased miR-124-3p inhibited the activity of mTOR signal transduction by targeting PDE4B, thereby inhibiting neuronal inflammation and promoting neurite growth (Se et al., 2017). Furthermore, the increase of miR-124-3p in microglia exosomes after TBI may inhibit neurons' autophagy and protect nerves from injury (Huang et al., 2018; Li et al., 2019a). However, Vuokila et al. (2020b) performed in situ hybridizations of miR-124-3p in temporal lobe autopsy samples of patients with TBI and found that miR-124-3p continued to decrease in TBI patients and may cause post-injury neurodegeneration and inflammatory responses. Although the expression and effect of miR-124-3p have been studied, the present study is the first to examine the effect of miR-124-3p on the interaction between glial cells. We found that overexpression of miR-124-3p alleviated the microglia- and astrocyte-mediated inflammatory response. This finding indicates that overexpression of miR-124-3p plays an active role in the treatment of TBI.

A previous study revealed that HOXA11-AS functioned as a competitive endogenous RNA through sponging miRNA, thus repressing miRNA-mediated functions (Cui et al., 2017). For example, a higher level of HOXA11-AS has been found in glioma tissue compared with the adjacent normal tissue, and has also been associated with poorer survival and prognosis of patients with glioma. Moreover, HOXA11-AS has been reported to sponge miR-140-5p and reverse miR-140-5p-mediated anti-tumor effects (Cui et al., 2017). Notably, miR-124-3p has also been found to be regulated by lncRNAs. For instance, one study found that miR-124-3p attenuated re-oxygenation-induced cell apoptosis and upregulation of proinflammatory mediators, and was negatively regulated by lncRNA regulator of reprogramming (Liang et al., 2019). Interestingly, several studies have revealed that HOXA11-AS sponges miR-124-3p, thereby modulating the progression of several diseases, including calcium oxalate crystal-induced renal inflammation (Li et al., 2020), keloid formation (Jin et al., 2020), and glioma (Yang et al., 2018). In this study, HOXA11-AS and miR-124-3p expression were negatively correlated in the brain lesions of TBI rats. Functionally, HOXA11-AS reduced miR-124-3p-mediated anti-inflammatory effects in microglia-astrocyte interaction.

MDK, a growth factor with neurotrophic and neurite growth activity, is usually expressed in ischemic areas during the acute phase of cerebral infarction in rats (Yoshida et al., 2014). In TBI, MDK is highly expressed, while down-regulation of MDK reduces tissue infiltration of microglia/macrophages and changes their polarization state, thereby reducing neuroinflammation and reducing neurological function after TBI (Takada et al., 2020). In the present study, we found that MDK was also markedly upregulated in the cerebral cortex of TBI rats. Our *in vitro* experiment revealed that knocking down MDK not only mitigated TLR4/NF-κB and inflammatory cytokine expression in microglia, but also repressed microglia-mediated astrocyte activation. This indicates that MDK serves as a proinflammatory mediator in microglia and astrocytes by activating the TLR4/NF-κB pathway. Conversely, a recent study demonstrated that the lncRNA/miRNA axis participates in the expression regulation of MDK (Duan et al., 2020). Namely, ZFAS1 inhibits miR-624, which acts as an upstream modulator of MDK, thus activating the extracellular regulatory protein kinase/c-Jun N-terminal kinase/P38 pathway and promoting the occurrence of hepatocellular carcinoma (Duan et al., 2020). Based on the above findings, we explored the function of HOXA11-AS/miR-124-3p and MDK in TBI. We found that miR-124-3p targeted the 3'-untranslated region of MDK mRNA. Moreover, the overexpression of miR-124-3p was found to reduce MDK expression, while upregulating HOXA11-AS enhanced MDK levels. Hence, HOXA11-AS regulates the inflammatory response of TBI through the MDK/TLR4/NF-κB signaling pathway by sponging miR-124-3p.

However, this study has several limitations that should be overcome in the future studies. First, limited rats were used for *in vivo* assay, and more animal experiments are needed to confirm the effects of HOXA11-AS in TBI progression. Second, the direct interaction between microglia and astrocytes in the TBI rat should be further investigated. Third, future studies should explore the clinical significance of the HOXA11-AS/miR-124-3p/MDK axis in patients with TBI.

Our paper provides a better understanding of the molecular mechanisms underlying TBI occurrence and development, which could facilitate the clinical diagnosis and treatment of TBI. Collectively, this study found that the overexpression of HOXA11-AS aggravates microglia/astrocyte activation in TBI. HOXA11-AS positively regulates the MDK signaling pathway and promotes the TBI-associated inflammatory response by promoting miR-124-3p.

References

Barros CS, Franco SJ, Müller U (2011) Extracellular matrix: functions in the nervous system. Cold Spring Harb Perspect Biol 3:a005108.

Ceci M, Mariano V, Romano N (2018) Zebrafish as a translational regeneration model to study the activation of neural stem cells and role of their environment. Rev Neurosci 30:45-66.

Cheng S, Zhang Y, Chen S, Zhou Y (2021) LncRNA HOTAIR participates in microglia activation and inflammatory factor release by regulating the ubiquitination of MYD88 in traumatic brain injury. J Mol Neurosci 71:169-177.

Cui Y, Yi L, Zhao JZ, Jiang YG (2017) Long noncoding RNA HOXA11-AS functions as miRNA sponge to promote the glioma tumorigenesis through targeting miR-140-5p. DNA Cell Biol 36:822-828.

De Luca C, Colangelo AM, Virtuoso A, Alberghina L, Papa M (2020) Neurons, glia, extracellular matrix and neurovascular unit: a systems biology approach to the complexity of synaptic plasticity in health and disease. Int J Mol Sci 21:1539.

Di Y, Wang Y, Wang X, Nie QZ (2021) Effects of long non-coding RNA myocardial infarction-associated transcript on retinal neovascularization in a newborn mouse model of oxygen-induced retinopathy. Neural Regen Res 16:1877-1881.

Duan R, Li C, Wang F, Han F, Zhu L (2020) The long noncoding RNA ZFAS1 potentiates the development of hepatocellular carcinoma via the microRNA-624/MDK/ERK/JNK/P38 signaling pathway. Onco Targets Ther 13:4431-4444.

Feeney DM, Boyeson MG, Linn RT, Murray HM, Dail WG (1981) Responses to cortical injury: I. Methodology and local effects of contusions in the rat. Brain Res 211:67-77.

Gong Y, Dai HS, Shu JJ, Liu W, Bie P, Zhang LD (2020) LNC00673 suppresses proliferation and metastasis of pancreatic cancer via target miR-504/ HNF1A. J Cancer 11:940-948.

Huang S, Ge X, Yu J, Han Z, Yin Z, Li Y, Chen F, Wang H, Zhang J, Lei P (2018) Increased miR-124-3p in microglial exosomes following traumatic brain injury inhibits neuronal inflammation and contributes to neurite outgrowth via their transfer into neurons. FASEB J 32:512-528.

Jin J, Jia ZH, Luo XH, Zhai HF (2020) Long non-coding RNA HOXA11-AS accelerates the progression of keloid formation via miR-124-3p/TGFβR1 axis. Cell Cycle 19:218-232.

Jin QS, Huang LJ, Zhao TT, Yao XY, Lin LY, Teng YQ, Kim SH, Nam MS, Zhang LY, Jin YJ (2018) HOXA11-AS regulates diabetic arteriosclerosis-related inflammation via PI3K/AKT pathway. Eur Rev Med Pharmacol Sci 22:6912-6921.

Kabadi SV, Stoica BA, Loane DJ, Luo T, Faden AI (2014) CR8, a novel inhibitor of CDK, limits microglial activation, astrocytosis, neuronal loss, and neurologic dysfunction after experimental traumatic brain injury. J Cereb Blood Flow Metab 34:502-513.

Lam D, Enright HA, Cadena J, Peters SKG, Sales AP, Osburn JJ, Soscia DA, Kulp KS, Wheeler EK, Fischer NO (2019) Tissue-specific extracellular matrix accelerates the formation of neural networks and communities in a neuron-glia co-culture on a multi-electrode array. Sci Rep 9:4159.

Li D, Huang S, Yin Z, Zhu J, Ge X, Han Z, Tan J, Zhang S, Zhao J, Chen F, Wang H, Lei P (2019a) Increases in miR-124-3p in microglial exosomes confer neuroprotective effects by targeting FIP200-mediated neuronal autophagy following traumatic brain injury. Neurochem Res 44:1903-1923.

Li N, Yang M, Shi K, Li W (2017) Long non-coding RNA HOXA11-AS in human cancer: A meta-analysis. Clin Chim Acta 474:165-170.

Li Y, Yan G, Zhang J, Chen W, Ding T, Yin Y, Li M, Zhu Y, Sun S, Yuan JH, Guo Z (2020) LncRNA HOXA11-AS regulates calcium oxalate crystal-induced renal inflammation via miR-124-3p/MCP-1. J Cell Mol Med 24:238-249.

Li Z, Han K, Zhang D, Chen J, Xu Z, Hou L (2019b) The role of long noncoding RNA in traumatic brain injury. Neuropsychiatr Dis Treat 15:1671-1677.

Liang YP, Liu Q, Xu GH, Zhang J, Chen Y, Hua FZ, Deng CQ, Hu YH (2019) The lncRNA ROR/miR-124-3p/TRAF6 axis regulated the ischaemia reperfusion injury-induced inflammatory response in human cardiac myocytes. J Bioenerg Biomembr 51:381-392.

Liu Y, Fan X, Zhao Z, Shan X (2020) LncRNA SLC7A11-AS1 contributes to lung cancer progression through facilitating TRAIP expression by inhibiting miR-4775. Onco Targets Ther 13:6295-6302.

Long X, Yao X, Jiang Q, Yang Y, He X, Tian W, Zhao K, Zhang H (2020) Astrocyte-derived exosomes enriched with miR-873a-5p inhibit neuroinflammation via microglia phenotype modulation after traumatic brain injury. J Neuroinflammation 17:89.

Muramatsu T (2011) Midkine: a promising molecule for drug development to treat diseases of the central nervous system. Curr Pharm Des 17:410-423.

O'Connell GC, Smothers CG, Winkelman C (2020) Bioinformatic analysis of brain-specific miRNAs for identification of candidate traumatic brain injury blood biomarkers. Brain Inj 34:965-974.

Prada I, Gabrielli M, Turola E, Iorio A, D'Arrigo G, Parolisi R, De Luca M, Pacifici M, Bastoni M, Lombardi M, Legname G, Cojoc D, Buffo A, Furlan R, Peruzzi F, Verderio C (2018) Glia-to-neuron transfer of miRNAs via extracellular vesicles: a new mechanism underlying inflammation-induced synaptic alterations. Acta Neuropathol 135:529-550.

Se YB, Kim SH, Kim JY, Kim JE, Dho YS, Kim JW, Kim YH, Woo HG, Kim SH, Kang SH, Kim HJ, Kim TM, Lee ST, Choi SH, Park SH, Kim IH, Kim DG, Park CK (2017) Underexpression of HOXA11 is associated with treatment resistance and poor prognosis in glioblastoma. Cancer Res Treat 49:387-398.

Sharma R, Kambhampati SP, Zhang Z, Sharma A, Chen S, Duh EI, Kannan S, Tso MOM, Kannan RM (2020) Dendrimer mediated targeted delivery of sinomenine for the treatment of acute neuroinflammation in traumatic brain injury. J Control Release 323:361-375.

Takada S, Sakakima H, Matsuyama T, Otsuka S, Nakanishi K, Norimatsu K, Itashiki Y, Tani A, Kikuchi K (2020) Disruption of Midkine gene reduces traumatic brain injury through the modulation of neuroinflammation. J Neuroinflammation 17:40.

Tay Y, Rinn J, Pandolfi PP (2014) The multilayered complexity of ceRNA crosstalk and competition. Nature 505:344-352.

Vicente-Rodríguez M, Fernández-Calle R, Gramage E, Pérez-García C, Ramos MP, Herradón G (2016) Midkine is a novel regulator of amphetamine-induced striatal gliosis and cognitive impairment: evidence for a stimulus-dependent regulation of neuroinflammation by midkine. Mediators Inflamm 2016:9894504.

Vuokila N, Das Gupta S, Huusko R, Tohka J, Puhakka N, Pitkänen A (2020a) Elevated acute plasma miR-124-3p level relates to evolution of larger cortical lesion area after traumatic brain injury. Neuroscience 433:21-35.

Vuokila N, Aronica E, Korotkov A, van Vliet EA, Nuzhat S, Puhakka N, Pitkänen A (2020b) Chronic regulation of miR-124-3p in the perilesional cortex after experimental and human TBI. Int J Mol Sci 21:2418.

Winkler C, Yao S (2014) The midkine family of growth factors: diverse roles in nervous system formation and maintenance. Br J Pharmacol 171:905-912.

Witcher KG, Bray CE, Chunchai T, Zhao F, O'Neil SM, Gordillo AJ, Campbell WA, McKim DB, Liu X, Dziabis JE, Quan N, Eiferman DS, Fischer AJ, Kokiko-Cochran ON, Askwith C, Godbout JP (2021) Traumatic brain injury causes chronic cortical inflammation and neuronal dysfunction mediated by microglia. J Neurosci 41:1597-1616.

Wu J, He J, Tian X, Luo Y, Zhong J, Zhang H, Li H, Cen B, Jiang T, Sun X (2020) microRNA-9-5p alleviates blood-brain barrier damage and neuroinflammation after traumatic brain injury. J Neurochem 153:710-726.

Xue JY, Huang C, Wang W, Li HB, Sun M, Xie M (2018) HOXA11-AS: a novel regulator in human cancer proliferation and metastasis. Onco Targets Ther 9:4387-4393.

Yang J, Sun G, Hu Y, Yang J, Shi Y, Liu H, Li C, Wang Y, Lv Z, Niu J, Liu H, Shi X, Wang H, Li P, Jiao B (2019a) Extracellular vesicle lncRNA metastasis-associated lung adenocarcinoma transcript 1 released from glioma stem cells modulates the inflammatory response of microglia after lipopolysaccharide stimulation through regulating miR-129-5p/high mobility group box-1 protein axis. Front Immunol 10:3161.

Yang JX, Liu B, Yang BY, Meng Q (2018) Long non-coding RNA homeobox (HOX) A11-AS promotes malignant progression of glioma by targeting miR-124-3p. Neoplasma 65:505-514.

Yang LX, Yang LK, Zhu J, Chen JH, Wang YH, Xiong K (2019b) Expression signatures of long non-coding RNA and mRNA in human traumatic brain injury. Neural Regen Res 14:632-641.

Yang X, Chen Y, Li J, Chen L, Ren H, Liu Y, Zhang X (2019c) Hypertonic saline maintains coagulofibrinolytic homeostasis following moderate-to-severe traumatic brain injury by regulating monocyte phenotype via expression of lncRNAs. Mol Med Rep 19:1083-1091.

Yang Y, Ye Y, Kong C, Su X, Zhang X, Bai W, He X (2019d) MiR-124 enriched exosomes promoted the M2 Polarization of microglia and enhanced hippocampus neurogenesis after traumatic brain injury by inhibiting TLR4 pathway. Neurochem Res 44:811-828.

Yi M, Dai X, Li Q, Xu X, Chen Y, Wang D (2019) Downregulated lncRNA CRNDE contributes to the enhancement of nerve repair after traumatic brain injury in rats. Cell Cycle 18:2332-2343.

Yoshida Y, Sakakima H, Matsuda F, Ikutomo M (2014) Midkine in repair of the injured nervous system. Br J Pharmacol 171:924-930.

Yu Y, Cao F, Ran Q, Wang F (2017) Long non-coding RNA Gm4419 promotes trauma-induced astrocyte apoptosis by targeting tumor necrosis factor α. Biochem Biophys Res Commun 491:478-485.

Zhang Y, Wang J, Zhang Y, Wei J, Wu R, Cai H (2019) Overexpression of long noncoding RNA Malat1 ameliorates traumatic brain injury induced brain edema by inhibiting AQP4 and the NF-κB/IL-6 pathway. J Cell Biochem 120:17584-17592.

Zhang Z, Yu T, Geng W (2020) Long non-coding RNA CCHE1 participates in postoperative distant recurrence but not local recurrence of osteosarcoma possibly by interacting with ROCK1. BMC Musculoskelet Disord 21:462.